High-Pressure Phase Equilibria in the Binary System (Methane + 5-α-Cholestane)

Eckhard Flöter, Christof Brumm, Theodoor W. de Loos,* and Jakob de Swaan Arons

Delft University of Technology, Faculty of Chemical Engineering and Materials Science, Laboratory of Applied Thermodynamics and Phase Equilibria, Julianalaan 136, 2628 BL Delft, The Netherlands

In this paper, experimental data on the phase behavior of the binary system (methane + 5-α-cholestane) are presented. Experiments were carried out according to the synthetic method. The temperature range investigated was from 320 K to 450 K. The pressures applied did not exceed 250 MPa. Vapor−liquid equilibria have been measured for 18 different mixtures. Additionally, the melting curve of pure 5-α-cholestane and the course of the three-phase curve (solid 5-α-cholestane + liquid + vapor) was determined. The second critical end point was located at a temperature $T = (342.2 \pm 0.5)$ K, a pressure $p = (193.3 \pm 0.4)$ MPa, and a mole fraction of 5-α-cholestane in the critical fluid phase $x = 0.049 \pm 0.004$.

Introduction

Accumulations of oil and gas at depths greater than usual have been found and considered to be exploited in recent years. The increased reservoir depths account for a few characteristic properties of these reservoirs. On one hand the reservoir pressure and temperature are increased compared to normal depths. On the other hand also the composition of the fluids found in these so-called hyperbaric reservoirs is exceptional. The fluids being either light volatile oils or gas condensates are characterized by an asymmetrical compositional distribution. The simultaneous presence of large methane fractions, in excess of 60 mol %, and significant amounts of heavy-end hydrocarbons up to tetracontane not only cause high dew- and/or bubble-point pressures but also account for the possible precipitation of solid hydrocarbon phases during production and processing (Ungerer et al., 1995; Montel, 1993; Lagourette et al., 1994; Daridon et al., 1996).

In general, effective design, operation, and optimization of the production and processing of the reservoir fluids require accurate knowledge of the phase behavior of the fluid mixtures encountered. To get an insight into the phase behavior of reservoir fluids, very often the phase behavior of model systems, e.g., binary mixtures, is studied. The experimental data found in the literature related to binary asymmetric systems split into different categories. There are solubility data either of supercritical methane in heavy hydrocarbons to mimic the phase behavior of oils (Darwish et al., 1993; Malone and Kobayashi, 1990) or of heavy hydrocarbons in supercritical methane to get an insight into the possible deposition of waxes from natural gas, as, e.g., occurring in pipelines (Suleiman and Eckert, 1995). However, experimental fluid phase equilibrium data of asymmetric systems covering the range from a liquid state to gas state are scarce due to the high pressures encountered.

In our laboratory we studied the phase behavior of different asymmetric systems all composed of methane and a heavy hydrocarbon. The heavy components were tetracosane (Flöter et al., 1996), 1-phenyldodecane, phenanthrene, and 5-α-cholestane.

Binary mixtures of methane and saturated heavy hydrocarbons do not show strong molecular interactions. Nevertheless, fairly nonideal behavior is found for these systems at elevated pressures due to the significant differences in molecular size of the components. Neglecting the fact of possible polymorphism, the schematic high-temperature phase behavior of asymmetric (methane + hydrocarbon) systems is as shown in Figure 1. This type of phase behavior is characterized by the existence of a three-phase curve of the type (solid heavy hydrocarbon + liquid + vapor). This curve starts at the triple point of the pure heavy component. It is assumed that methane does not dissolve in the solid heavy component. The liquid phase becomes richer in methane with increasing pressure. Also, the vapor phase, starting from pure heavy component first becomes richer in methane. At a certain pressure the minimum concentration of the heavy component to allow retrograde condensation is reached and the vapor phase now becomes richer in heavy hydrocarbon with increasing pressure (Rijkers, 1991). At the so-called second critical end point, where a critical-fluid phase is in equilibrium

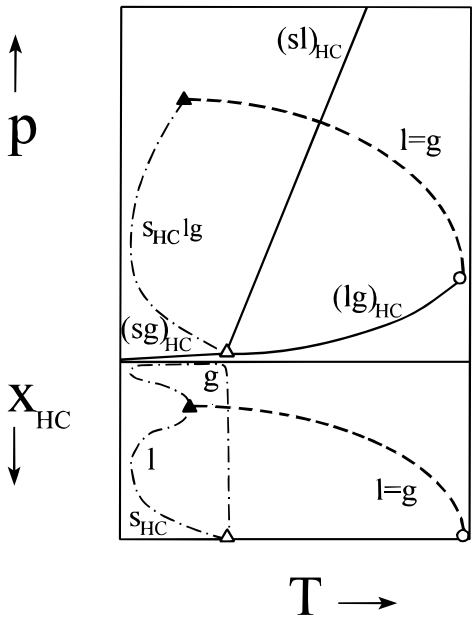

Figure 1. Schematic high-temperature phase behavior of asymmetric binary (methane + hydrocarbon (HC)) systems. Symbols: (○) pure component critical point; (△) pure component triple point; (▲) upper critical end point. Lines: (—) pure component phase boundary; (− − −) vapor−liquid critical curve; (− · −) (solid heavy hydrocarbon + liquid + vapor) three-phase curve.

* To whom correspondence should be addressed.

S0021-9568(96)00214-2 CCC: $14.00

Table 1. Melting Curve of Pure 5-α-Cholestane

T/K	*p*/MPa	*T*/K	*p*/MPa	*T*/K	*p*/MPa	*T*/K	*p*/MPa	*T*/K	*p*/MPa
449.83	212.85	419.50	145.85	401.67	108.55	385.95	69.99	364.73	24.60
441.15	193.25	417.74	141.85	400.99	105.81	382.57	63.25	362.95	19.96
432.02	173.10	409.91	125.55	394.80	90.90	377.59	51.48	359.23	13.35
425.45	158.85	408.37	123.57	393.58	87.80	370.57	36.12	358.93	11.46
423.94	155.65	405.86	117.55	386.15	71.65	366.72	27.72	353.15	≈0.1

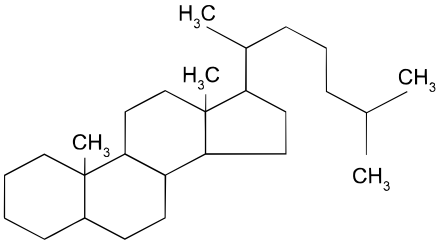

Figure 2. Schematic structure of 5-α-cholestane.

with a solid heavy hydrocarbon phase the vapor and the liquid branch of the three-phase curve (slg) merge. This critical end point is a point of intersection of the three-phase curve and the critical curve.

In this paper, experimental results on the phase behavior of the binary system (methane (A) + 5-α-cholestane (B)) and on the melting curve of pure 5-α-cholestane (CASRN 481-21-0, see also Figure 2) are presented. Vapor−liquid two-phase boundaries for 18 mixtures and the solid−liquid−vapor three-phase curve of the system have been studied. The temperature range investigated extends from about 320 K to 450 K, while the maximum pressure applied is less than 250 MPa.

Experimental Section

The methane used for the measurements was of ultra-high purity (99.995 mass %), supplied by Air Products. The 5-α-cholestane (CASRN 481-21-0) was supplied by Aldrich Chemie and had a stated purity of at least 99 mass %. DSC analyses of the 5-α-cholestane showed less than 0.5 mol % impurities, which were not further identified.

The high-pressure experiments were carried out using either a sapphire windowed autoclave (de Loos et al., 1980) or, at lower pressures ($p \leq 15$ MPa), a so-called Cailletet apparatus (de Loos et al., 1986). A detailed description of the two apparatus and the experimental procedure is given elsewhere (de Loos et al., 1980, 1986; van der Kooi et al., 1995). The general working principle of the two apparatus is the same. According to the synthetic method, the phase behavior of a sample of constant and known composition is determined for the temperature range of interest. The sample is enclosed in a half-open glass tube. The open end of the tube is submerged into mercury so that the mercury serves as a sealing and pressure transmitting fluid. By variation of the pressure the occurrence or disappearance of a phase can be induced. These changes of the state of the sample are visually detected. To prevent metastable states the procedure for dew- and bubble-point measurements is based on the detection of the disappearance of a phase with increasing pressure. For the measurements of the three-phase equilibrium points the transition from a (solid + liquid) or, depending on the overall composition of the sample, a (solid + vapor) two-phase state, to a (liquid + vapor) two-phase state was detected. The composition along the three-phase equilibrium curve can be found by the intersection of isoplethic vapor−liquid equilibrium curves with the three-phase equilibrium curve.

The coordinates of the second critical end point, where a solid 5-α-cholestane phase is in equilibrium with a critical-fluid phase, are determined indirectly. Since the second critical end point is located on the vapor−liquid critical curve, the composition of the critical-fluid phase has to be located between the composition of a mixture revealing dew-point behavior and of another mixture revealing bubble-point behavior. If these two mixtures do not differ too much in composition, their pressure and temperature coordinates at the respective three-phase equilibrium points should also almost coincide. This is so, because the three-phase curve ($s_B$lg) has at the second critical end point in the (T, x) as well as the (p, x) projection a relatively flat local maximum with respect to composition. Therefore, the pressure and temperature coordinates of the second critical end point and the three-phase equilibrium points of the neighboring mixtures practically coincide.

For both apparatus stability of temperature is established by means of temperature-controlled baths. The actual temperature measurement is carried out with Pt-100 resistance thermometers connected to resistance bridges (ASL F-16). This allows the determination of transition temperatures with an accuracy better than ±0.04 K. The pressures are measured and kept constant with dead weight gauges. The uncertainty of the pressure reading was at most ±0.08 MPa.

Since the measurements on top of the above given hardware accuracies also depend on the visibility of the transition under consideration, the vapor−liquid equilibrium measurements justify an accuracy better than ±0.15 MPa. This is so, because for the detection of a dew point the presence of the last liquid droplets is impeded by the dome of the mercury meniscus inside the sample containment. For the measurements of the three-phase (solid 5-α-cholestane + liquid + vapor) equilibrium points the visibility of the phase transition only allows us to state an accuracy of ±0.5 MPa. Due to the slope of the three-phase curve it was not always possible to determine a phase transition accurately by pressure variation. In such cases the equipment was used in an isobaric mode. This yields a much less accurate determination of the transition temperature to an accuracy of ±0.5 K. The points of the melting curve of pure 5-α-cholestane were determined with an accuracy of ±0.2 MPa. The accuracy of the given compositions is better than ±0.004 for the mole fraction of cholestane with a tendency to decrease with decreasing cholestane mole fraction.

It was also intended to measure the solubility of solid 5-α-cholestane in supercritical methane over a wide concentration range. However, due to supersaturation, the generation of a solid 5-α-cholestane phase from binary mixtures could not be induced in a reproducible way. Supersaturation was observed at pressures of even 50 MPa above and at temperatures of more than 10 K below the equilibrium conditions.

Results

The vapor−liquid phase behavior of the binary system (methane (A) + 5-α-cholestane (B)) was determined for 18 binary mixtures. The temperature range investigated was from 320 to 450 K. Further, the melting curve of pure 5-α-cholestane was measured. In Table 1 the experimental findings for the melting curve are listed. The experimental vapor−liquid equilibrium data are given in Table 2. In

Table 2. Vapor−Liquid Equilibrium Data for (Methane (A) + 5-α-Cholestane (B))[a]

T/K	*p*/MPa	*T*/K	*p*/MPa	*T*/K	*p*/MPa	*T*/K	*p*/MPa	*T*/K	*p*/MPa
				$x_B = 0.005$ (d.p.)					
330.45	139.28	360.72	136.28	400.67	97.06	433.82	84.85		
341.47	130.08	376.40	108.26	408.78	93.86	445.35	81.05		
353.34	121.47	385.47	103.86	420.63	89.45	458.23	77.05		
				$x_B = 0.010$ (d.p.)					
335.72	168.70	368.13	139.28	404.15	117.47	439.28	101.86	470.74	90.45
346.67	157.29	379.11	131.68	415.52	111.87	451.70	97.06		
358.12	147.09	391.13	124.47	427.14	106.66	463.02	93.05		
				$x_B = 0.021$ (d.p.)					
325.47	207.52	354.12	171.90	383.38	147.09	417.53	126.67	451.78	111.27
335.80	192.71	361.43	164.70	395.00	139.28	429.25	120.87	462.67	107.06
347.17	179.51	373.17	154.69	406.15	132.68	441.19	115.67		
				$x_B = 0.030$ (d.p.)					
325.53	214.53	359.25	172.90	385.11	151.49	418.30	131.28	453.25	115.47
336.47	198.92	370.69	162.70	396.28	143.88	431.15	124.87	464.31	111.07
348.31	184.31	377.38	157.09	407.35	136.68	441.51	120.27		
				$x_B = 0.041$ (d.p.)					
325.45	215.33	358.17	174.70	395.29	145.89	429.49	127.27	462.89	113.07
336.29	200.12	370.57	163.90	407.42	138.28	440.57	122.07		
347.35	186.71	381.13	155.49	419.23	132.18	451.60	117.67		
				$x_B = 0.046$ (d.p.)					
339.41	196.45	393.72	146.95	435.12	124.75				
357.18	176.25	432.58	125.95	458.63	115.15				
				$x_B = 0.052$ (b.p.)					
307.58	249.35	329.25	210.52	352.59	180.61	371.09	163.70	395.27	146.09
312.02	240.04	335.15	202.02	357.81	175.60	375.92	159.69	407.47	138.68
317.06	230.74	339.34	196.52	357.50	176.00	384.93	152.89	420.92	131.48
321.64	222.73	344.00	190.71	361.87	171.80	386.71	151.69	425.72	129.28
325.75	215.73	348.60	185.51	367.05	167.00	389.30	149.89	438.96	123.12
				$x_B = 0.075$ (b.p.)					
325.07	213.53	357.29	174.50	385.67	151.29	415.42	133.48	445.16	120.07
336.52	198.52	370.11	163.10	393.59	146.09	427.56	127.68	455.29	115.87
348.56	183.11	377.03	157.29	404.17	139.48	435.30	123.87	462.76	113.07
				$x_B = 0.099$ (b.p.)					
324.98	201.12	358.24	165.30	391.90	141.68	425.72	124.92	453.27	114.07
336.33	187.41	371.20	155.29	402.85	135.68	435.35	120.92	467.99	109.06
348.12	174.90	379.49	149.09	414.77	129.93	441.37	118.27		
				$x_B = 0.153$ (b.p.)					
325.41	163.10	360.72	136.28	393.63	119.67	428.76	107.46	460.47	98.86
336.51	153.09	369.53	131.48	404.35	115.67	443.94	103.06		
348.36	144.29	379.78	126.07	416.52	111.47	452.11	100.86		
				$x_B = 0.202$ (b.p.)					
324.23	129.48	361.40	111.07	393.96	99.66	426.58	91.35	454.11	85.85
338.03	122.07	374.17	106.26	405.24	96.46	433.60	89.85	462.84	84.25
349.05	116.87	382.27	103.46	415.35	93.86	441.36	88.25		
				$x_B = 0.290$ (b.p.)					
326.06	86.05	357.42	78.05	389.85	72.24	426.49	67.64	461.77	63.64
337.82	82.85	366.43	76.04	402.42	70.44	437.56	66.24		
348.76	79.85	377.40	74.24	415.18	68.84	452.47	64.64		
				$x_B = 0.399$ (b.p.)					
325.77	49.23	357.68	47.03	388.61	45.63	423.34	44.23	462.64	42.63
336.68	48.43	368.52	46.43	399.35	45.03	435.95	43.83		
347.66	47.63	377.53	46.03	412.21	44.63	448.65	43.23		
				$x_B = 0.400$ (b.p.)					
392.97	44.50	414.46	44.10	445.70	42.90	464.58	42.10		
403.85	44.30	430.96	43.50	458.09	42.50				
				$x_B = 0.499$ (b.p.)					
330.67	29.82	344.24	30.02	362.42	30.02	395.76	30.17	434.55	30.07
335.05	29.82	348.24	30.02	373.90	30.02	407.71	30.17	448.41	29.97
339.71	30.02	353.09	30.02	384.53	30.22	421.48	30.17	465.42	29.87
				$x_B = 0.625$ (b.p.)					
330.43	16.41	357.55	17.21	397.36	18.01	434.71	18.41		
339.61	16.61	366.57	17.41	409.34	18.21	447.87	18.41		
348.78	17.01	384.42	17.81	420.67	18.41	463.20	18.61		
				$x_B = 0.750$ (b.p.)					
341.28	8.98	378.28	9.76	413.30	10.25	443.28	10.45	483.71	10.55
353.28	9.27	393.27	10.10	423.32	10.25	453.25	10.55		
365.28	9.56	403.30	10.06	433.28	10.35	468.27	10.55		
				$x_B = 0.896$ (b.p.)					
333.23	2.97	363.27	3.27	408.37	3.56	453.24	3.76		
343.28	3.07	378.27	3.37	423.27	3.66	470.27	3.76		
353.29	3.17	393.27	3.46	438.30	3.66				

[a] (d.p.) indicates dew-point measurements. (b.p.) indicates bubble-point measurements.

Table 3. (Solid 5-α-Cholestane + Liquid + Vapor) Three-Phase Equilibrium Data in the (Methane + 5-α-Cholestane) System

T/K	*p*/MPa	*T*/K	*p*/MPa	*T*/K	*p*/MPa	*T*/K	*p*/MPa	*T*/K	*p*/MPa
341.90	190.21	338.95	147.69	331.20	91.65	332.85	33.62	344.96	9.58
341.60	185.21	338.85	146.69	329.54	80.65	332.85	28.62	345.26	8.30
340.64	173.95	336.59	130.18	329.48	47.63	341.37	12.31	347.47	6.30
340.13	160.19	335.47	122.67	330.48	40.62	342.52	11.01	349.51	4.15
339.09	150.69	332.86	102.66	331.14	35.62	344.27	10.08	353.15	<0.1

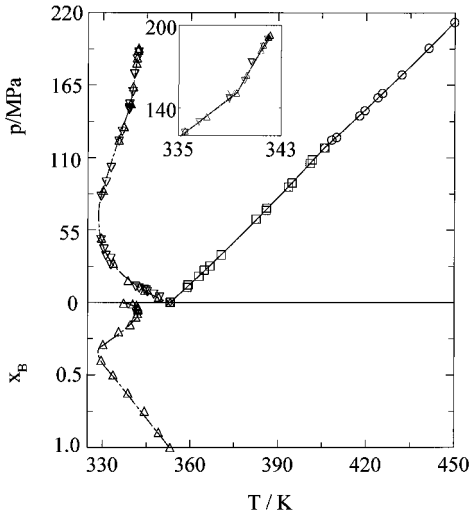

Figure 3. (*p*, *T*) and corresponding (*x*, *T*) projection of the $s_B$lg three-phase curve of the (methane (A) + 5-α-cholestane (B)) system and the melting curve of pure 5-α-cholestane: (− · −) (solid 5-α-cholestane + liquid + vapor) three-phase curve; (▽) direct measurements of *p* and *T*; (△) determined by intersection of vle and $s_B$lg direct; (—) melting curve of pure 5-α-cholestane; (□) low-pressure form of solid 5-α-cholestane; (○) high-pressure form of solid 5-α-cholestane.

addition, the course of the three-phase (solid 5-α-cholestane + liquid + vapor) equilibrium curve in a (*p*, *T*) projection was determined. The pressure and temperature coordinates are given in Table 3.

From the experimental data given in Table 1 and shown in Figure 3 one can see that the average slope (d*p*/d*T*) of the melting curve of pure 5-α-cholestane is approximately 2.35 MPa/K. This is much smaller than for *n*-alkanes of similar size. Further, it is found that the slope of the melting curve shows a discontinuity at a temperature of about $T = 406$ K and a pressure of about $p = 118$ MPa.

Figure 4 shows the primary experimental vapor−liquid equilibrium data. A few isopleths ($x_B = 0.075$, 0.041, 0.030) were omitted for the sake of clarity of the figure. The figure reveals that with decreasing mole fraction of 5-α-cholestane in the liquid phase the slopes $(\partial p/\partial T)_x$ of the bubble-point curves are decreasing. For a mixture with a mole fraction of 5-α-cholestane of 0.5 the bubble-point pressure is almost independent of temperature. It is over a temperature range of 135 K constant to within 0.3 MPa. For dew-point curves the evolvement of the slope $(\partial p/\partial T)_x$ with respect to composition is inverse to the one of the bubble-point curves.

On the basis of the primary experimental data isobaric or isothermal data sets can be derived. To do so, low-degree polynomials were fitted to the experimental data to allow interpolations. In Figure 5 four isothermal vapor−liquid two-phase envelopes are shown. The figure clearly reveals that the vapor−liquid critical composition is practically constant in the temperature range investigated. Further, the critical pressure is monotonously decreasing. The isotherm of 340 K crosses the three-phase curve (solid 5-α-cholestane + liquid + vapor) twice. This indicates that the high-pressure part ($p \geq 164.0$ MPa) and the low-

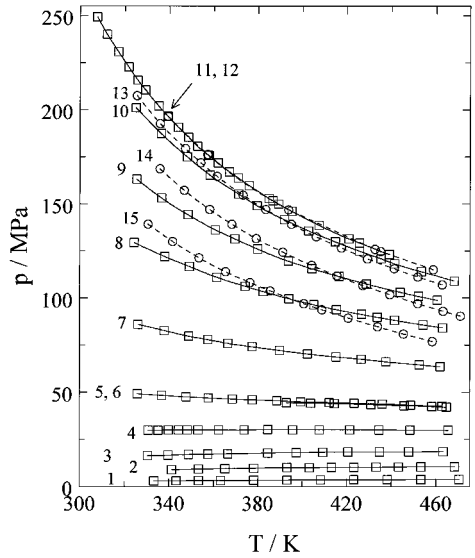

Figure 4. Vapor−liquid equilibrium in the system (methane (A) + 5-α-cholestane (B)): phase boundary pressure as a function of temperature at constant 5-α-cholestane mole fraction. (□) Bubble point (b.p.): (1) $x_B = 0.896$; (2) $x_B = 0.750$; (3) $x_B = 0.625$; (4) $x_B = 0.499$; (5) $x_B = 0.400$; (6) $x_B = 0.399$; (7) $x_B = 0.290$; (8) $x_B = 0.202$; (9) $x_B = 0.153$; (10) $x_B = 0.099$; (11) $x_B = 0.052$. (○) Dew point (d.p.): (12) $x_B = 0.046$; (13) $x_B = 0.021$; (14) $x_B = 0.010$; (15) $x_B = 0.005$.

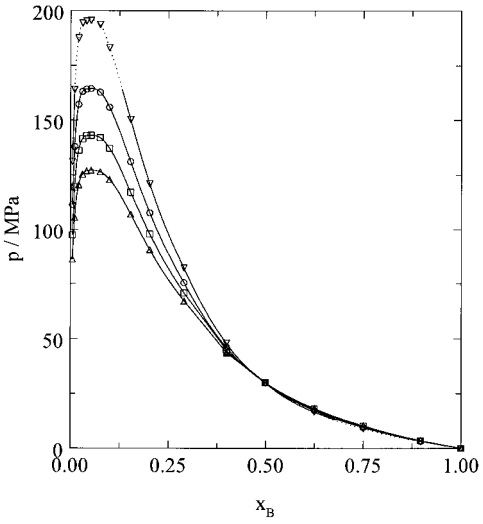

Figure 5. Pressure versus 5-α-cholestane mole fraction x_B diagram of the vapor−liquid equilibrium of the (methane (A) + 5-α-cholestane (B)) system: (▽) 340 K; (○) 370 K; (□) 400 K; (△) 430 K. The dotted curves indicate metastable equilibria.

pressure part ($p \leq 13.1$ MPa) of this curve represent vapor−liquid equilibria which are metastable with respect to solid−fluid equilibria. These metastable parts are depicted as dotted curves in Figure 5.

The (*p*, *T*) and corresponding (*x*, *T*) projections of the (solid 5-α-cholestane + liquid + vapor) three-phase curve shown in Figure 3 were constructed on the basis of the directly measured three-phase equilibrium points and the isoplethic vapor−liquid equilibrium curves. Starting from

the triple point of pure 5-α-cholestane the curve runs with increasing mole fraction of methane in the liquid phase to higher pressures and lower temperatures. The three-phase curve shows a clear temperature minimum at a pressure $p = (65.0 \pm 15.0)$ MPa, a temperature $T = (328.5 \pm 1.2)$ K, and a composition of the liquid phase of $x_B = 0.35 \pm 0.05$. Above this pressure the temperature of the three-phase equilibrium points is increasing with increasing pressure. Similar patterns for the course of the three-phase curve were also found for asymmetric (methane + *n*-alkane) systems (Glaser et al., 1985; van der Kooi et al., 1995; Flöter et al., 1996). In the high-pressure part of the three-phase curve, at a pressure of about 150 MPa, an abrupt change in the slope of the three-phase curve is found (see insert in Figure 3). This is probably caused by a change of the crystal structure of solid 5-α-cholestane. The coordinates of the second critical end point, where solid 5-α-cholestane is in equilibrium with a critical fluid phase, were determined as described above. They are found to be $T = (342.2 \pm 0.5)$ K, $p = (193.3 \pm 0.4)$ MPa, and $x_B = 0.049 \pm 0.004$.

Discussion

The type of phase behavior found for the system (methane (A) + 5-α-cholestane (B)) fits into the patterns of types of phase behavior found for systems composed of methane and a saturated hydrocarbon. The coordinates of the second critical end point of the (methane + 5-α-cholestane) system differ from the ones of a system composed of methane and an *n*-alkane with the same number of carbon atoms, i.e. 27. The latter coordinates are determined on the basis of correlations given elsewhere (Flöter et al., 1995). It is found that the pressure (193.3 to 115.0 MPa) and the mole fraction of the heavy component in the fluid phase (0.049 to 0.037) are higher in the system incorporating 5-α-cholestane. Further, it should be noted that the shape of the three-phase curve differs from the ones found in the homologous series of (methane + *n*-alkane) systems (Flöter et al., 1995). The temperature minimum $\{T = (328.5 \pm 1.2)$ K, $p = (65.0 \pm 15.0)$ MPa, $x_B = 0.35 \pm 0.05\}$ found is more pronounced for the 5-α-cholestane system than for *n*-alkane systems. It is striking that the composition of the liquid phase at the temperature minimum of the three-phase curve, within the stated accuracies, equals the ones found in asymmetric (methane + *n*-alkane) systems (van der Kooi et al., 1995). The average slope (dp/dT) of the melting curve of pure 5-α-cholestane is with 2.35 MPa/K, much smaller than for comparable *n*-alkanes. To relate the different slope of the melting curve to either different volumetric or entropic effects is speculative since insufficient information on the properties of pure 5-α-cholestane is available. The discontinuities found in the slope (dp/dT) of the melting curve of pure 5-α-cholestane at $p \approx 115$ MPa and in the slope (dp/dT) of the three-phase curve at $p \approx 150$ MPa give reason to assume the presence of more than one form of solid 5-α-cholestane. These kinds of discontinuities were earlier explained by polymorphism (Schneider, 1978; Flöter et al., 1996).

Literature Cited

Daridon, J. L.; Xans, P.; Montel, F. Phase Boundary Measurement on a Multi-Paraffins System. *Fluid Phase Equilib.* **1996**, *117*, 241−248.

Darwish, N. A.; Fathikaljahi, J.; Gasem, K. A. M.; Robinson, R. L., Jr. Solubility of Methane in Heavy Normal Paraffins at Temperatures from 323 to 423 K and Pressures up to 10.7 MPa. *J. Chem. Eng. Data* **1993**, *38*, 44−48.

de Loos, Th. W.; Wijen, A. J. M.; Diepen, G. A. M. Phase Equilibria and Critical Phenomena in Fluid (Propane + Water) at High Pressures and Temperatures. *J. Chem. Thermodyn.* **1980**, *12*, 193−204.

de Loos, Th. W.; van der Kooi, H. J.; Ott, P. L. Vapour-Liquid Critical Curve of the System Ethane + 2-Methyl-Propane. *J. Chem. Eng. Data* **1986**, *31*, 166−168.

Flöter, E.; de Loos, Th.W.; de Swaan Arons, J. Hyperbaric Reservoir Fluids: High-Pressure Phase Behaviour of Asymmetric Methane + n-Alkane Systems. *Int. J. Thermophys.* **1995**, *16*, 185−194.

Flöter, E.; de Loos, Th.W.; de Swaan Arons, J. Solid-Fluid and Vapor-Liquid Equilibria in Binary Reservoir Model Fluids. *Fluid Phase Equilib.* **1996**, *117*, 153−159.

Flöter, E.; de Loos, Th.W.; de Swaan Arons, J. High Pressure Solid-Fluid and Vapour-Liquid Equilibria in the System (Methane + Tetracosane). *Fluid Phase Equilib.*, in press.

Glaser, M.; Peters, C. J.; van der Kooi, H. J.; Lichtenthaler, R. N. Phase Equilibria of (Methane + n-Hexadecane) and (p, V_m, T) of n-Hexadecane. *J. Chem. Thermodyn.* **1985**, *17*, 803−815.

Jenkins, E. W. *The Polymorphism of Elements and Compounds*; Menthuen Studies in Science; Menthuen Educational Ltd, London, 1973.

Lagourette, B.; Daridon, J. L.; Gaubert, J. F.; Xans, P. Experimental determination of ultrasonic speeds in (methane + propane) (g) and in (methane + octane) (g) at high pressures. *J. Chem. Thermodyn.* **1994**, *26*, 1051−1061.

Malone, P. V.; Kobayashi, R. Light Gas Solubility in Phenanthrene: The Hydrogen-Phenanthrene and Methane-Phenanthrene Systems. *Fluid Phase Equilib.* **1990**, *55*, 193−205.

Montel, F. High Pressure High Temperature Reservoir Fluid Properties. Contribution to the 13th European Seminar on Applied Thermodynamics, Carre-le-Rouet, France, 10th−12th of June, 1993.

Rijkers, M. P. W. M. Retrograde Condensation of Lean Natural Gas: PhD Thesis, Delft University Press, 1991.

Schneider, G. M. Specialist Periodical Reports, Chemical Thermodynamics Vol. 2; The Chemical Society: London 1978.

Suleiman, D.; Eckert, C. A. Phase Equilibria of Alkanes in Natural Gas Systems: Part1 Alkanes in Methane. *J. Chem. Eng. Data* **1995**, *40*, 2−12.

Ungerer, P.; Faissat, B.; Leibovici, C.; Zhou, H.; Behar, E.; Moracchini, G.; Courcy, J. P. High pressure-high temperature reservoir fluids: investigation of synthetic condensate gases containing a solid hydrocarbon. *Fluid Phase Equilib.* **1995**, *111*, 287−311.

van der Kooi, H. J.; Flöter, E.; de Loos Th. W. High Pressure Phase Equlibria of $\{(1-x)\ CH_4 + x\ CH_3(CH_2)_{18}CH_3\}$. *J. Chem. Thermodyn.* **1995**, *27*, 847−861.

Received for review June 25, 1996. Accepted October 8, 1996.[⊗]

JE960214P

[⊗] Abstract published in *Advance ACS Abstracts,* November 15, 1996.